Article

Not peer-reviewed version

A Mechanically Tunable,Fatigue-Resistant, and Reusable Plasticizable Dual-Network Hydrogel

Zhuangzhuang Xin , Wei Xu * , Yaping Zhang , Yongwei Yao , Defa Liu , Jilu Duan , Wanxiang He

Posted Date: 12 June 2023

doi: 10.20944/preprints202306.0853.v1

Keywords: hydrogel; polyvinyl alcohol; hydrogen bonding; mechanics; stress; reusability; recycling

Article

A Mechanically Tunable, Fatigue-Resistant, and Reusable Plasticizable Dual-Network Hydrogel

Zhuangzhuang Xin [1], Wei Xu [1,*], Yaping Zhang [2], Yongwei Yao [3], Defa Liu [2], Jilu Duan [2] and Wanxiang He [2]

[1] Faculty of Civil Engineering and Mechanics, Kunming University of Science and Technology, Kunming 650500, China
[2] Faculty of Science, Kunming University of Science and Technology, Kunming 650500, China
[3] Faculty of Mechanical and Electrical Engineering, Kunming University of Science and Technology, Kunming 650500, China
* Correspondence: 13354909706@163.com

Abstract: Natural cellulose hydrogels have been widely used to enhance mechanical properties. However, existing natural fiber composite hydrogels are not reusable, limiting their potential applications. To address this issue, we designed and prepared a polyvinyl alcohol/glycerol /bamboo microfibril double network tough hydrogel using a simple method. The bamboo microfibril and polyvinyl alcohol form a tight and rigid network through hydrogen bonding, improving mechanical properties. The prepared polyvinyl alcohol/glycerol/bamboo microfibril double network tough hydrogel has the advantages of reusability and fatigue resistance. Furthermore, both the elastic modulus and toughness of the hydrogel increase with increasing bamboo microfibril content. We also demonstrated that the hydrogel can be recast after cyclic compression, maintaining its recyclability, stability, and certain stiffness and toughness. Our study highlights the potential of hydrogels for controllable mechanical properties, fatigue resistance and shows that polyvinyl alcohol/glycerol/bamboo microfibril hydrogel has broad value for plasticity and reuse.

Keywords: hydrogel; polyvinyl alcohol; hydrogen bonding; mechanics; stress; reusability; recycling

1. Introduction

Hydrogels, three-dimensional cross-linked networks of polymer chains, are a class of biomimetic soft materials with tunable physical and chemical properties. Due to the synergistic effect of their hydrophilic networks and water interactions, hydrogels exhibit solid-like mechanical properties and transport properties for water molecules, which have attracted wide attention in agriculture for drought resistance and moisture retention, drug delivery, personal care products, biomaterials for adsorption, and tissue engineering [1–5]. However, most hydrogels are inherently fragile and susceptible to collapse and damage during use, limiting their application prospects [6–12]. To address this issue, researchers have designed and constructed a series of functional hydrogels with high strength and toughness, including double network gels, topological gels, slip ring gels, and nanocomposite gels [13–20]. Among them, Dual-Network hydrogels(DN hydrogels) are considered promising materials due to their excellent mechanical performance and energy dissipation capacity. Meanwhile, different type of DN hydrogels offer enhanced mechanical strength, durability, and superior performance compared to each individual network alone [21–23]. Based on the types of bonds involved, dual-network hydrogels can be categorized into three main types [24,25]. The first type of hydrogels is the Physical Crosslinked DN hydrogels, which consist of two physically crosslinked networks formed through non-covalent interactions such as hydrogen bonds, van der Waals forces and hydrophobic interactions. This type of DN hydrogels formed by physical cross-linking are reversible and can be disassembled or reassembled by altering the environmental conditions of the hydrogel, such as temperature, solvent, or pH. Therefore, Physical Crosslinke DN hydrogels exhibit high plasticity, reversibility, and reshaping capabilities. The second type of hydrogels is the Chemical Crosslinked DN hydrogels, this type of double-network hydrogel consists of two chemically cross-linked networks, each network being cross-linked by covalent bonds. This type of DN hydrogel can be produced by adding different metal or non-metal ions and inorganic compounds to form irreversible chemical reactions, resulting in a densely structured and mechanically superior DN hydrogel. The third type is the Hybrid Crosslinked DN hydrogels, where one network is physically crosslinked and the other is chemically crosslinked through covalent bonds. This combination enables the hydrogels to possess both the reversible properties of physical crosslinking and the stability and strength of chemical crosslinking [26–32]. By utilizing different types of networks, dual-network hydrogels harness the advantages of each bonding type to achieve remarkable properties and broaden their applications in various fields [33–38].

Since the groundbreaking research by Gong et al. on DN hydrogels [39], various novel hydrogels based on the principles of DN hydrogels have been extensively reported, greatly expanding the research value and prospects of DN hydrogels. Despite the exciting progress in this field, covalently crosslinked DN hydrogels exhibit inherent limitations such as irreversible bond breakage during compression or stretching [40–46]. While the mechanical properties of covalently crosslinked DN hydrogels can be significantly enhanced, challenges remain in terms of controllability of mechanical performance, weak fatigue resistance, limited reshaping and self-healing capabilities, and the inability for secondary utilization [47–50].

Although physically cross-linked double-network DN hydrogels exhibit inferior mechanical properties compared to chemically cross-linked DN hydrogels, they possess several advantages such as plasticity, controllable mechanical performance, and fatigue resistance [51–54]. Therefore, the synthesis of DN hydrogels utilizing physically cross-linked reversible sacrificial bonds has been a key focus of research. Even when subjected to external forces that lead to the rupture of internal non-covalent bonds, physically cross-linked DN hydrogels can exhibit a certain capacity for secondary utilization and repeated use due to the ability of non-covalent bonds (such as intermolecular hydrogen bonds, van der Waals forces or hydrophobic interactions) to reconnect [55–59].

Therefore, this study aims to develop a novel DN hydrogel using physical crosslinking, which incorporates two types of physical crosslinking networks - a flexible network and a rigid network - both formed through hydrogen bonding (non-covalent interactions) to construct the DN hydrogel with superior pliability, reusability, and fatigue resistance.

In addition, incorporating nanoscale fillers into the gel system is also an effective strategy for producing rigid hydrogels [11,17,64]. Despite the significant progress made in DN hydrogels materials using these strategies, most DN hydrogels lack the ability to be recycled and reused, limiting their biodegradability and recyclability [63–68]. Therefore, it is desirable to construct a recyclable hydrogel as a substitute for disposable hydrogels, by adding natural fiber materials such as cotton, hemp, and bamboo to improve the mechanical properties of hydrogels [30–34]. As a hydrogel filler, natural fibers can increase cross-linking density to enhance gel mechanical properties and promote the use of hydrogels [74,76,77].

Among various natural fibers, bamboo fiber provides ample opportunities for large-scale production and manufacturing due to its widespread growth range worldwide, fastest growth rate, strong texture, and excellent adsorption capacity derived from its raw material - bamboo [79–85]. Bamboo microfibril (BMF), which is the main component of bamboo, is also the primary reason for the superior toughness and mechanical properties of bamboo raw fiber [86,87]. BMF (one type of bamboo fiber) is not only biodegradable and cost-effective but also possesses advantages such as antibacterial properties, moisture absorption, breathability, adsorption, and environmental friendliness, making it an excellent candidate for a wide range of applications. Methods for extracting bamboo cellulose include mechanical, chemical, and combined mechanical-chemical methods. Purified bamboo fibers extracted from different species of bamboo are not only used to produce bamboo fiber-reinforced composites (BFRP) but also serve as fiber materials for hydrogels and aerogels [11,13,88–91]. For instance, Guimaraes M et al. synthesized starch/PVA/BMF hydrogels, while Xuexia Zhang et al. prepared PVA/BMF hydrogels [92,93]. Dan Ren et al. developed a bamboo nanocellulose composite film for food packaging, and Dinh Duc Nguyen et al. investigated the properties of micrometer-sized white bamboo fiber-based silane-cellulose aerogels [94,95]. Xuexia

Zhang et al. fabricated bamboo cellulose (MFC) aerogels with different contents, and K W Prasetiyo et al. studied paper pulp composite materials made from PVA and bleached or unbleached bamboo pulp fibers (Bambusa vulgaris) for food packaging and other applications [96,97].

Therefore, constructing a biomass-based DN hydrogel as a substitute for petroleum-based synthetic polymers to prepare recyclable hydrogels is highly desirable due to their biodegradability, biocompatibility, non-toxicity, and abundance in nature. To improve the mechanical properties of DN hydrogels, biomass-based cellulose fibers can be incorporated and cross-linked physically or chemically to form a network structure.

In this study, bamboo microfibril were prepared from bamboo through a physical-chemical method. The novel DN hydrogels were then synthesized by incorporating BMF particles into a polyvinyl alcohol (PVA) and glycerol (GC) base, and varying the mass fraction of BMF particles. The resulting hydrogels with different mechanical properties were obtained by high-temperature mixing and F-T processing. In addition to their controllable mechanical properties, these composite hydrogels possess advantages such as low-temperature flexibility, excellent compressibility, good recyclability, and high reusability.

2. Materials and methods

2.1. Materials

Polyvinyl alcohol (PVA) 1799 with a polymerization degree of 1700 and alcoholysis degree of 99% was purchased from China National Pharmaceutical Group Chemical Reagent Co., Ltd. (Suzhou, China). Glycerol (GC) was obtained from Shandong Deinuo Medical Technology Co., Ltd. (Dezhou, China). Moso bamboo powder (purity 99%) was sourced from Anhua County, Yiyang City, Hunan Province, China. Anhydrous sodium sulfite (Na_2SO_3) was procured from Tianjin Fengchuan Chemical Reagent Technology Co.,Ltd. (Tianjin, China). H_2O_2 solution and NaOH standard solution were purchased from Fuzhou Feijing Biological Technology Co., Ltd. (Fuzhou, China). Deionized water (H_2O) used in the experiments was obtained from Qianjing Environmental Protection Technology Co., Ltd. (Guangzhou, China). All reagents were of analytical grade and used without further purification.

2.2. Preparation of BMF Microparticle

Polishing bamboo into powder, sieving it through a 300-mesh screen, and immersing it in a mixture of NaOH (2.5mol/L) and Na_2SO_3 (0.4mol/L) with a molar ratio of 1:2 are effective methods for removing lignin and hemicellulose from the bamboo powder. The resulting suspension, containing bamboo microfibrils, was subjected to constant heating at 90℃ for 5 hours. After allowing the suspension to settle for 1 hour, the residual solid at the bottom was extracted and washed with deionized water until the pH of the washing solution reached neutrality (pH=7) at room temperature. Subsequently, the solid was dried and immersed in a 100mL solution of H_2O_2 (2.5mol/L) and subjected to constant heating at 90℃ for 1.5 hours. The resulting powder was washed with deionized water until the pH of the washing solution reached neutrality (pH=7) at room temperature and then dried to obtain bamboo micro-fibril particles, referred to as BMF.

2.3. Preparation of Physically Crosslinked PVA/GC/BMF Hydrogel

In order to obtain PVA based hydrogels that are physically crosslinked and tough, F-T method was used [98,99]. 30g of PVA was added to 60 g of deionized water and stirred magnetically at 95°C until a transparent viscous liquid was obtained. The entire heating and stirring process was carried out in a sealed water bath to prevent water evaporation. Then, 30 g of gelatinous cellulose (GC) was added to the PVA aqueous solution, and the mixture was heated and stirred magnetically for 3 hours to obtain a homogeneous solution. Subsequently, a mixed solution containing different concentrations of bamboo microfibrils (BMF) was added, and the mixture was heated and stirred magnetically for another hour. The resulting mixture was poured into a hollow cylindrical polytetrafluor-oethylene (PTFE) mold with a diameter of 20 mm, a height of 30 mm, and a thickness of 2 mm. The mold was sealed with transparent glass plates (SiO_2) and placed in a freezer at -38°C for 12 hours. After freezing, the mold was thawed at room temperature for 12 hours, and the process was repeated five times using the same freeze-thaw (F-T) method. The prepared PVA/GC/BMF hydrogel was then immersed in deionized water for at least one week to remove impurities. After reaching swelling equilibrium, the PVA/GC/BMF hydrogel was stored in deionized water for further experimentation. Six PVA based hydrogels with different components or templates were prepared according to the above method. The material ratio of each group is shown in Table 1, and the hydrogel preparation strategy is shown in Figure 1.

Table 1. PVA/GC/BMF hydrogels with different contents and ratios.

Number	Ratio of BMF	PVA	H_2O	GC	BMF
1	0.0wt%	10g	60g	30g	0.00g
2	0.5wt%	10g	60g	30g	0.50g
3	1.5wt%	10g	60g	30g	1.52g
4	2.5wt%	10g	60g	30g	2.56g
5	3.5wt%	10g	60g	30g	3.63g
6	5.0wt%	10g	60g	30g	5.26g

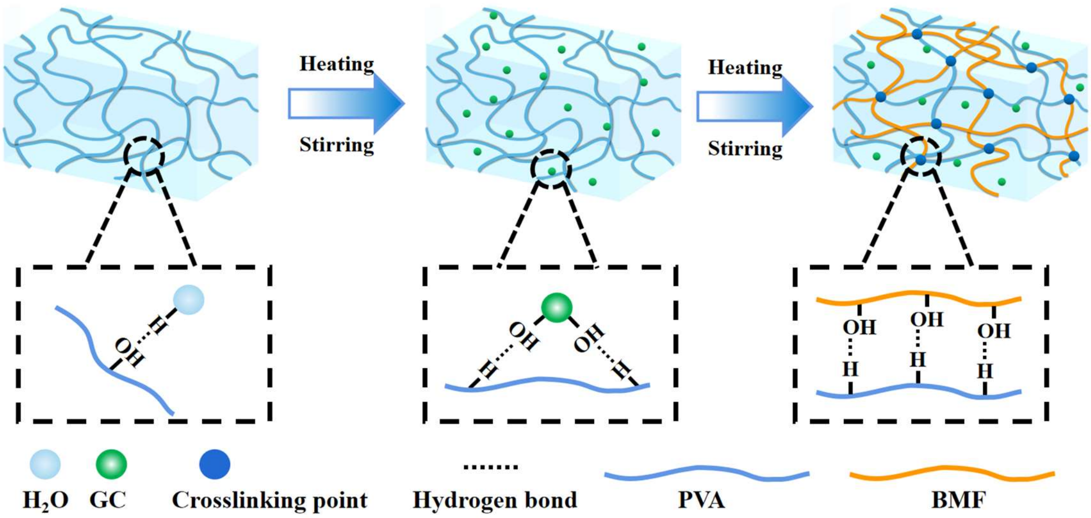

Figure 1. (a) Hydrogel preparation strategy flow chart.

2.4. Characteristics

2.4.1. Mechanical performance testing Compression and low cycle fatigue testing

The fabricated strip-shaped hydrogel is illustrated in Figure 2(a). The strip hydrogel was subsequently subjected to bending (Figure 2(b)), torsion (Figure 2(c)), and tensile deformation (Figure 2(e)-(f)), demonstrating its initial evidence of toughness and extensibility. To further evaluate the mechanical properties of the hydrogel, we used an MTG universal testing machine (MTS810, Germany) and a 1000NS column pressure sensor (Dexton Sensing System Engineering Co., Ltd., Shenzhen, China), compression and low-cycle fatigue tests were performed on cylindrical water gel samples (sample size: 20 mm diameter × 20 mm height). The fabricated cylindrical hydrogel is depicted in Figure 2(d).To remove excess surface moisture, the water gel samples were placed on a sterile bench and gently wiped with a tissue until the surface was dry before being compressed under unconstrained conditions. Compression was performed at a rate of 30 mm/min and a compression amount equal to 50% of the sample height. Each group of samples was subjected to 2000 cycles of compression. Stress-strain and low-cycle fatigue curves were recorded for each compression cycle. The compression modulus was determined from the initial slope of the stress-strain curve. The elastic modulus was the average value of three independent test samples of the same kind. After 2000 cycles

Preprints.org (www.preprints.org) | NOT PEER-REVIEWED | Posted: 12 June 2023 doi:10.20944/preprints202306.0853.v1

of compression for each of the six different water gel samples, the surface dust was washed off with deionized water, and the samples were placed in deionized water for 48 h. Then, each group was melted and recast, mixed and heated in a water bath for 2 hours, and poured into a polytetrafluoroethylene (PTFE) cylindrical mold with a diameter of 20 mm, a height of 30 mm, and a thickness of 2 mm. The mold was sealed with transparent glass plates (SiO2) and placed in a freezer at -38°C for 12 hours. The mold was then thawed at room temperature for 12 hours and subjected to the same F-T method for five repetitions. The recast PVA/GC/BMF water gel was immersed in deionized water for at least 1 week to remove impurities. After the gel reached swelling equilibrium, the same compression and low-cycle fatigue tests were performed on the six different BMF-containing water gel samples, each subjected to 2000 cycles of compression. The compression modulus was measured in the ran ge of 5%-15% compression rate, and stress-strain curves were plotted for different numbers of cyclic loads.

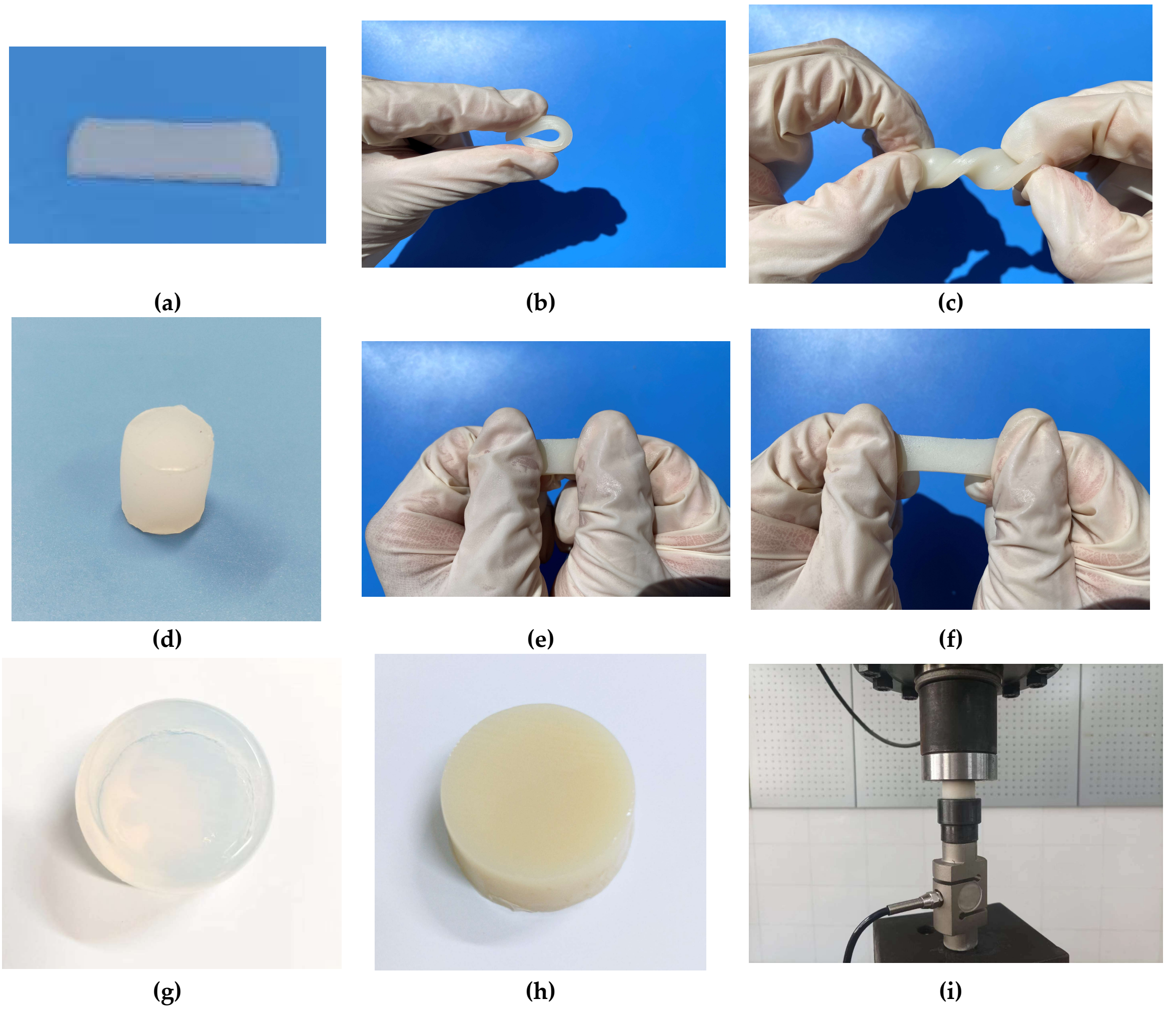

Figure 2. **(a)** Bending test of 5.0wt% BMF/PVA/GC strip hydrogel **(b)** Bending test of 5.0wt% BMF/PVA/GC strip hydrogel **(c)** Torsion test of 5.0wt% BMF/PVA/GC strip hydrogel **(d)** Tensile test of 5.0wt% BMF/PVA/GC column hydrogel **(e-f)** 5.0wt% BMF/PVA/GC gel **(g)** The prepared 0.0wt% BMF/PVA/GC cylindrical hydrogel **(h)** The prepared 5.0wt% BMF/PVA/GC cylindrical hydrogel **(i)** Mechanical compression test of hydrogel.

2.4.2. Scanning electron microscopy and infrared spectroscopy testing

The cross-sections of PVA/GC/BMF hydrogels with different concentrations (0wt%, 0.5wt%, 1.5wt%) were treated with sputter coating and imaged using a high-resolution field emission scanning electron microscope (Nova-Nano450, Germany) at an acceleration voltage of 5 kV. Additionally, the infrared spectra of PVA/GC/BMF hydrogels with different concentrations (0wt%,

Preprints.org (www.preprints.org) | NOT PEER-REVIEWED | Posted: 12 June 2023 doi:10.20944/preprints202306.0853.v1

1.5wt%, 2.5wt%, and 3.5wt%) were obtained using an infrared spectrometer (Bruker ALPHA, Germany) with a resolution of 4 cm-1 and a scanning range of 4000-500 cm^{-1}, and the spectra were collected by averaging 16 scans.

2.5. Results and Discussion

2.5.1. Design strategy and structural characteristics of hydrogel

The first flexible network of PVA chains and GC molecules was formed through hydrogen bonding, while the second rigid network was created by the entanglement of BMF chains and PVA chains via hydrogen bonding. Based on the chemical properties of BMF, PVA, and GC, it is hypothesized that hydrogen bonding occurs between GC and PVA chains, as each GC molecule contains three free hydroxyl groups, and each PVA chain has free hydrogen atoms. In addition, when BMF is combined with PVA and GC, physical cross-linking via hydrogen bonding occurs between the free hydrogen atoms on PVA chains and the hydroxyl groups on BMF molecules, forming intermolecular hydrogen bonds.

To confirm this hypothesis, we first conducted infrared spectroscopy tests on PVA/GC hydrogels with different GC contents (0wt%, 5wt%, and 30wt%) before adding BMF, as shown in Figure 3 (a); According to Figure 3 (a), we observed that a prominent absorption peak at 3386-3400 cm^{-1} in the functional group region (4000 cm^{-1}-1500 cm^{-1}) signifies the occurrence of hydroxyl group stretching vibrations within the molecule. Furthermore, the presence of a broad peak at this region indicates the formation of crosslinks and intermolecular hydrogen bonding between PVA and GC. Remarkably, the peak values at 0.0wt% GC/PVA, 5.0wt% GC/PVA, and 30.0wt% GC/PVA were measured as 3385 cm^{-1}, 3387 cm^{-1}, and 3399 cm^{-1}, respectively. These results demonstrate that as the mass fraction of GC increases, the peak value of the broad peak progressively increases, leading to a stronger intensity of the absorption peak and a gradual rise in the number of intermolecular hydrogen bonds formed; The absorption peak observed at 2947-2967 cm^{-1} indicates the anti-symmetric saturated stretching vibrations of the C-H bonds within the CH_2 groups after crosslinking between PVA and GC. Additionally, the weak absorption peak at 2105-2190 cm^{-1} suggests irregular vibrations of intermolecular carbon-carbon double bonds. Moreover, the strong absorption peak observed at 1645-1649 cm^{-1} indicates the stretching vibrations of carbon-carbon double bonds associated with the presence of alkenes.

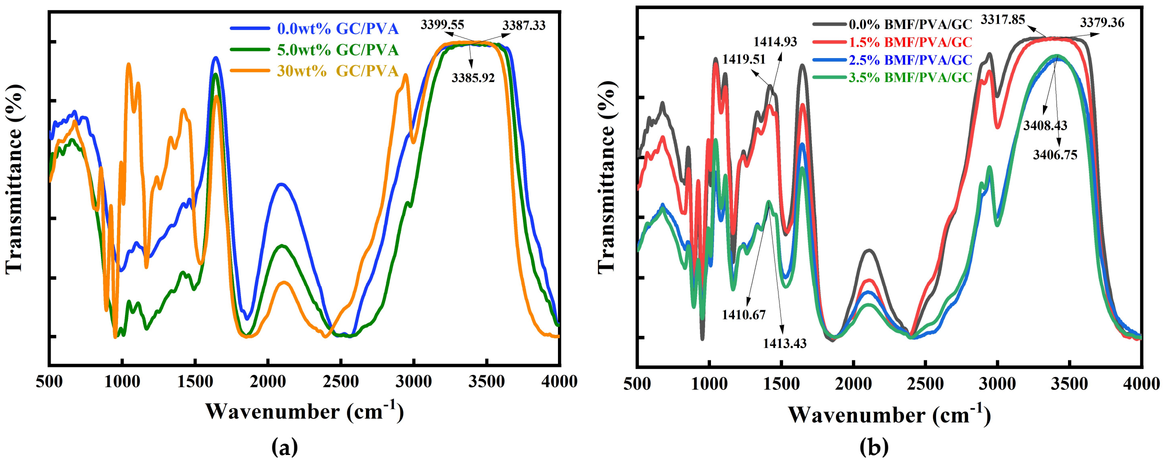

Figure 3. (a) Different GC content infrared spectroscopy testing **(b)** Different BMF content infrared spectroscopy testing **(f)** 0.5wt% BMF/PVA/GC surface SEM image.

Meanwhile, we investigated the incorporation of different quality grades of BMF into PVA/GC hydrogels, as shown in Figure 3 (b); According to Figure 3 (b), in the functional group region (4000 cm^{-1}-1500 cm^{-1}), a strong absorption peak was observed at 3318-3409 cm^{-1}, indicating the stretching vibrations of the hydroxyl groups within the molecule. Interestingly, within the same range, a broad peak was observed for 0.0 wt% BMF/PVA/GC and 1.5 wt% BMF/PVA/GC, while sharp peaks were observed for 2.5 wt% BMF/PVA/GC and 3.5 wt% BMF/PVA/GC. This phenomenon can be attributed to the presence of four free hydroxyl groups (-OH) in each BMF molecule $(C_6H_{10}O_5)_n$. As the BMF content increases, the free hydrogen ions within the molecule combine with the free hydroxyl groups, resulting in the formation of intermolecular hydrogen bonds. Consequently, an increased amount of BMF leads to a decrease in the quantity of free hydrogen ions outside the molecule and an increase in the number of free hydroxyl groups. Therefore, the increase in free hydroxyl groups is responsible for the transition from a broad peak to sharp peaks. Furthermore, within this range, the peak values were measured at 3317 cm^{-1}, 3379 cm^{-1}, 3406 cm^{-1}, and 3408 cm^{-1} for 0.0 wt% BMF/GC/PVA, 1.5 wt% BMF/GC/PVA, 2.5 wt% BMF/GC/PVA, and 3.5 wt% BMF/GC/PVA, respectively. These findings indicate that as the mass fraction of BMF increases, the intensity of the absorption peak also increases, suggesting the formation of a greater number of intermolecular hydrogen bonds between BMF and PVA. The absorption peak observed at 2942-2945 cm^{-1} can be attributed to the stretching vibrations of the C-H bonds within the molecule. Additionally, the weak absorption peak at 2102-2106 cm^{-1} suggests irregular vibrations of intermolecular carbon-carbon double bonds. Furthermore, the strong absorption peak observed at 1642-1646 cm^{-1} indicates the stretching vibrations of carbon-carbon double bonds associated with the presence1of1alkenes.In addition, SEM images of the cross-sections of three different BMF-containing hydrogels are shown in Figure 4(a)-(c). We observed that in the cross-section of the 0wt% BMF hydrogel, the PVA chain structure was arranged in an orderly and parallel manner. With the addition of BMF, the PVA chain structure was combined with the BMF chain structure, and the cross -section- al structure gradually changed from an orderly and parallel arrangement to an unordered chain structure. This indicated that entanglement occurred between the molecular chains and the fusion of multiple molecules.

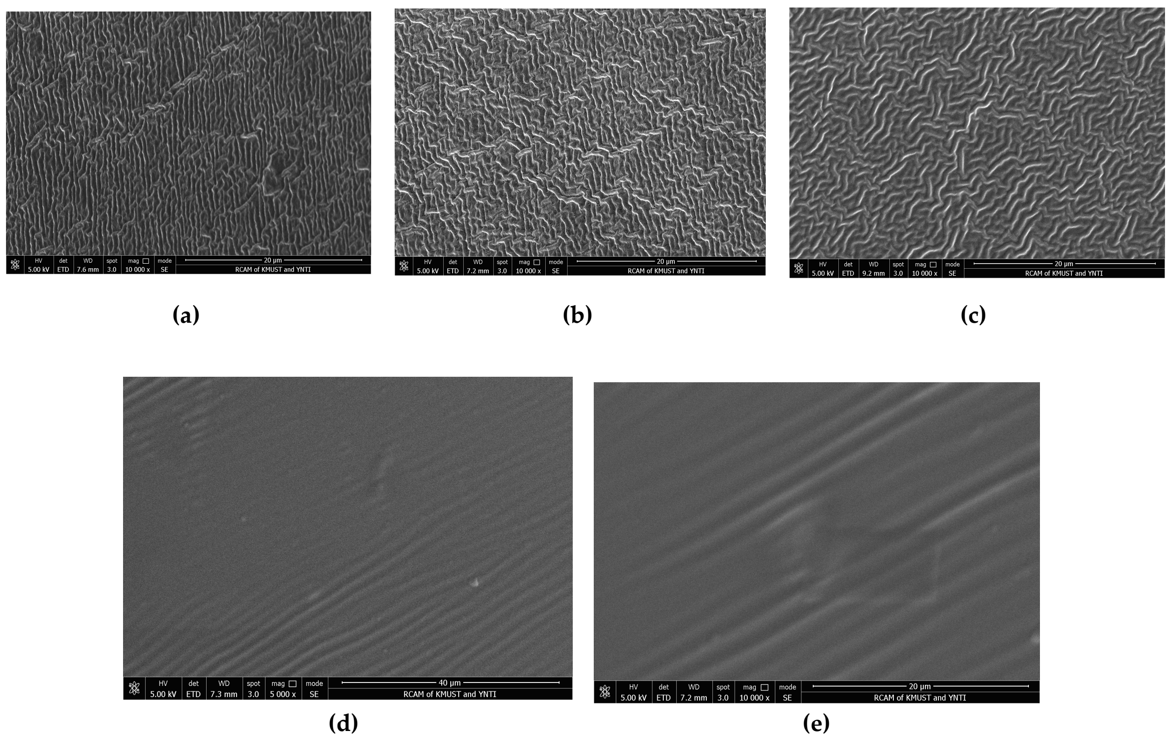

Figure 4. (a) 0wt% BMF/PVA/GC SEM image **(b)** 0.5wt% BMF/PVA/GC SEM image **(c)** 1.5wt% BMF/PVA/GC SEM image **(d)** 0.0wt% BMF/PVA/GC surface SEM image **(e)** 0.5wt% BMF/PVA/GC surface SEM image.

Furthermore, Figure 4(d) presents the SEM image of the surface of the BMF hydrogel with 0.0 wt%, while Figure 4(e) illustrates the SEM image of the surface of the BMF hydrogel with 1.5 wt%. By comparing these two images, it is evident that the addition of a small amount of BMF has no significant impact on the surface morphology of the hydrogel. The hydrogel surface exhibits no noticeable protrusions or distinct bright or dark regions, indicating that the incorporation of a small amount of BMF enhances the mechanical performance of the hydrogel without compromising its surface smoothness.

In summary, our comparative analysis of two distinct types of hydrogels and seven different infrared spectroscopy curves provides evidence that both PVA with GC and PVA with BMF are crosslinked through hydrogen bonding, thereby confirming our hypothesis. Furthermore, SEM testing confirms that the addition of BMF enables the formation of a compact internal structure within the hydrogel, while maintaining the smoothness of the hydrogel surface.

2.5.2. Mechanical property test of hydrogel

To investigate the anti-fatigue performance of hydrogels, we conducted 2000 cycles of compression tests on each type of hydrogel without any interruption. Stress-strain curves were obtained at the 1st, 500th, 1000th, 1500th, and 2000th cycles(Figure 5(a)-(f)), After the first cycle, the hysteresis height and elastic modulus of the hydrogels decreased with increasing cycle number. The trend of decreasing hydrogel toughness stabilized after multiple cycles. The possible reason is that the internal network structure of the hydrogel is partially damaged during cyclic loading, and energy dissipation is due to the elasticity of the covalently cross-linked hydrogel network and the reversibility of the dynamic hydrogen bonds within the hydrogel. After removing the strain, the covalently cross-linked network contracts elastically, and the hydrogen bonds, as sacrificial bonds, reform, which helps to partially recover the hydrogel network.

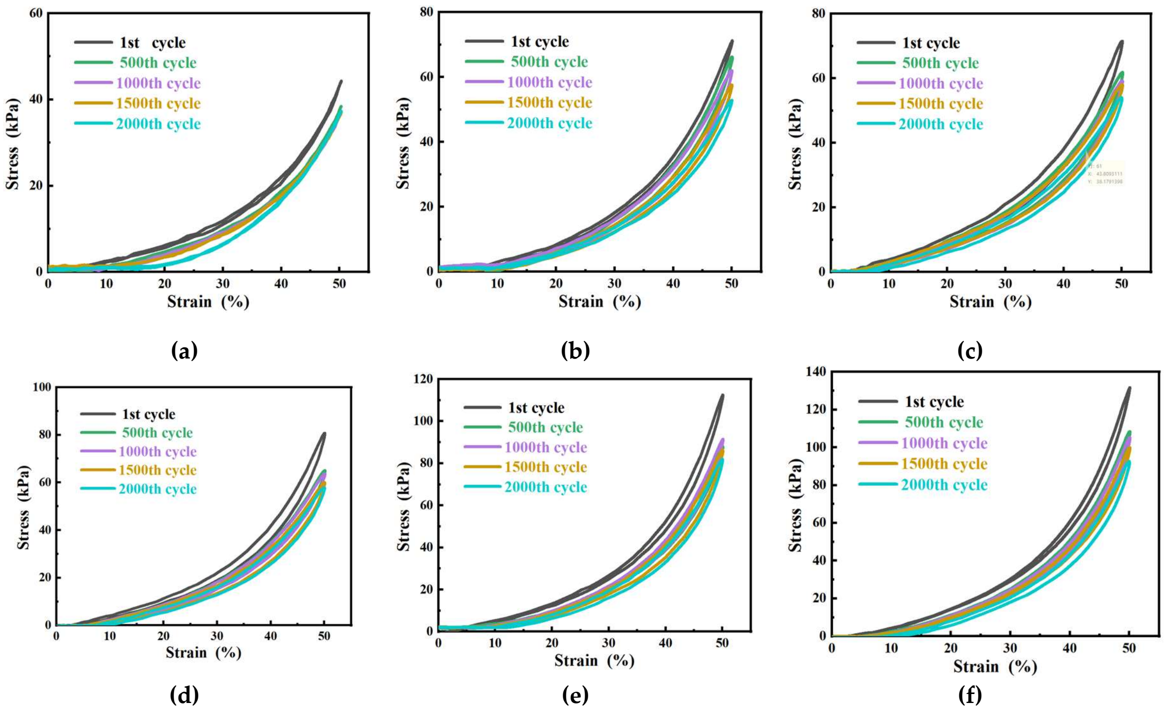

Figure 5. (a) 0.0wt% BMF/PVA/GC low cycle fatigue test **(b)** 0.5wt% BMF/PVA/GC low cycle fatigue test **(c)** 1.5wt% BMF/PVA/GC low cycle fatigue test **(d)** 2.5wt% BMF/PVA/GC low cycle fatigue test **(e)** 3.5wt% BMF/PVA/GC low cycle fatigue test **(f)** 5.0wt% BMF/PVA/GC low cycle fatigue test.

We found that compared with the cyclic loading curves of other gels, all types of hydrogels exhibited significant hysteresis and energy dissipation. The energy dissipation of 0wt% BMF/PVA/GC decreased with increasing cycle number(Figure 7(f)). The reason for this phenomenon may be that the hydrogen bonds between PVA and GC are damaged under high strain, and this interaction cannot be immediately restored before the subsequent cycles, leading to a small amount of energy consumption and a gap between each cycle's loading curve. For 0wt% BMF hydrogel, except for the maximum stress (~44.3 kPa) and elastic modulus (~30.3 kPa) (Figure 7(a) and(b)), which

Preprints.org (www.preprints.org) | NOT PEER-REVIEWED | Posted: 12 June 2023 doi:10.20944/preprints202306.0853.v1

were the minimum values, the cyclic loading curves of the gel without BMF almost overlapped for each cycle(Figure 5(a)), indicating that the energy dissipation of the gel without BMF was less. The flexible network formed by 0wt% BMF/PVA/GC gel had limited effectiveness in dissipating energy. As BMF was added, the area under the cyclic loading curve gradually increased, indicating that the energy dissipation ability of the hydrogel was significantly enhanced.

Compared with the stress loading curves of PVA/GC gel(Figure 6(f)), the cyclic loading curves of BMF-containing hydrogel showed obvious hysteresis at higher strain rates, indicating that energy dissipation occurred during cyclic loading. The reason for energy dissipation may be that the hydrogen bonds between the two long chain molecules, PVA and BMF, in the gel undergo strong interaction, and hydrogen bonds at the crosslinking points break to absorb external energy during large deformation. Additionally, after each cycle, the hydrogel containing BMF returned to its original state and was not crushed, possibly because the hydrogen bonds that were cross-linked between the polymer matrix and BMF were damaged and broken under high strain, and the interactions between hydrogen bonds could not be immediately restored before the subsequent cycles, leading to the consumption of energy within the hydrogel.

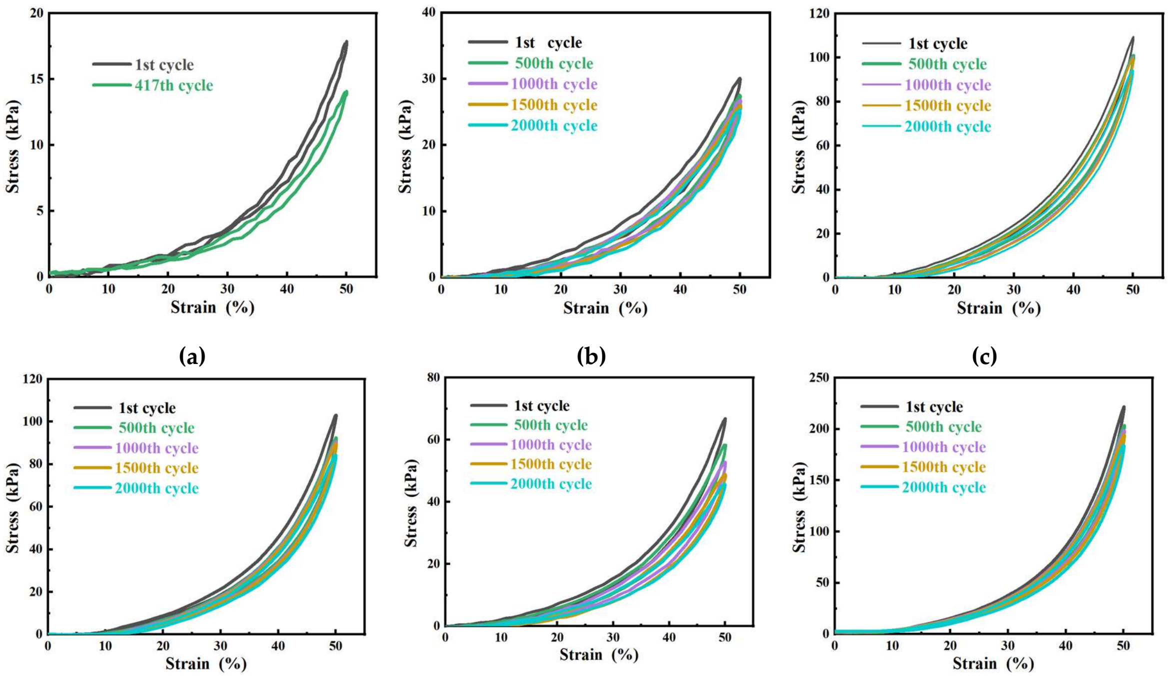

(a) (b) (c)

(d) (e) (f)

Figure 6. (a) Low cycle fatigue test at 0.0wt% BMF/PVA/GC after recasting **(b)** Low cycle fatigue test at 0.5wt% BMF/PVA/GC after recasting **(c)** Low cycle fatigue test at 1.5wt% BMF/PVA/GC after recasting **(d)** Low cycle fatigue test at 2.5wt% BMF/PVA/GC after recasting **(e)** Low cycle fatigue test at 3.5wt% BMF/PVA/GC after recasting **(f)** Low cycle fatigue test at 5.0wt% BMF/PVA/GC after recasting.

Under the same strain conditions, the compressive strength and Young's modulus of water gel increase as the content of BMF increases (Figure 7(e)). The highest compressive strength was observed in 5.0wt% BMF/PVA/GC hydrogel. At 50% strain, the compressive stress of 5.0wt% BMF/PVA/GC hydrogel (~118.0 kPa) was 2.7 times higher than that of PVA/GC hydrogel (~44.3 kPa), indicating that BMF effectively enhances the mechanical strength of PVA/GC hydrogel. Furthermore, the Young's modulus of 5.0wt% BMF/PVA/GC hydrogel (~78.1 kPa) was 2.6 times higher than that of PVA/GC hydrogel (~30.3 kPa) and 2.0 times higher than that of 0.5wt% BMF/PVA/GC hydrogel (~37.7 kPa), indicating that BMF plays a key role in enhancing the gel network structure of PVA/GC.

Moreover, with the increase of BMF content, the improvement of gel mechanical properties is accompanied by the stabilization of the gel internal structure. The cyclic loading curves from 0% to

5% become smoother, and the strong interaction between BMF and PVA long-chain molecules plays a crucial role in making the stress-strain curve of the hydrogel more uniform and enhancing the mechanical properties. The SEM of 1.5wt% BMF/PVA/GC hydrogel shows an irregular linear network structure (Figure 4(c)). This is due to the hydrogen bonding between the free hydroxyl group of BMF and the free hydrogen ion of the PVA chain molecule, which acts as a physical cross-linking point in the double-network hydrogel, intertwining and integrating the long chains of BMF and PVA to achieve a compact and stable internal network, avoiding the instability and collapse of pore structures caused by the sublimation of water molecules inside the gel during the freeze-thaw process.

Compared with the initial gel mechanical properties, we found that the curves of 0% BMF/PVA/GC and 0.5wt% BMF/PVA/GC exhibit large fluctuations (Figure 7(a)-(b)).

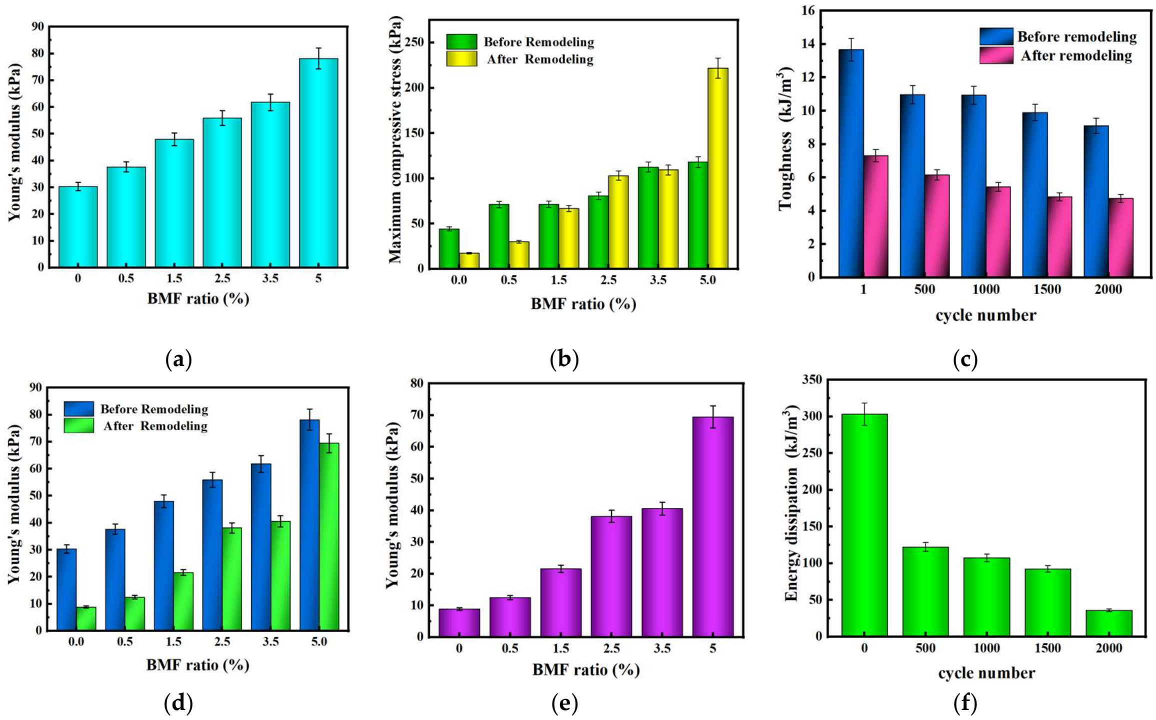

Figure 7. (a) Hydrogel Young's Modulus Histogram **(b)** Hydrogel Maximum Pressure Stress Histogram **(c)** Hydrogel Toughness Diagram **(d)** Hydrogel Young's Modulus Comparison Diagram **(e)** Hydrogel Young's Modulus Histogram after Recasting **(f)** 0.0wt% BMF/PVA/GC Hydrogel Energy Dissipation Variation Diagram.

The reason for the fluctuation of these curves is that when the BMF content is low, GC in the hydrogel makes the PVA molecular chain structure loose, acting as a dispersant, resulting in a relatively loose gel structure. Meanwhile, during the freeze-thaw process of gel remolding, water molecules inside the gel absorb heat during the process of transitioning from low temperature to room temperature, causing some water molecules to sublimate and creating pores within the gel, leading to an unstable and non-uniform internal structure of the gel and causing fluctuations in the cyclic loading curve. This indicates that the mechanical properties of the gel significantly decrease without the addition of BMF, and the recyclability of the 0% BMF hydrogel is weak since it fractures after 418 cycles of compression (Figure 7(a)).

Furthermore, In this study, we observed that the recast hydrogel still exhibits energy dissipation characteristics during cyclic loading. The breaking of hydrogen bonds and energy absorption during cyclic loading ensure the smooth progress of energy dissipation. Although the elastic modulus and maximum compressive stress of the recast hydrogel are reduced compared to those of the same type of hydrogel before recasting (Figure 7(c)), the elastic modulus and maximum compressive stress of the recast water-based hydrogel still increase with the increase of BMF content (Figure 7(e)). As BMF is continuously added, the maximum compressive stress of the recast hydrogel gradually increases. The maximum compressive stress of 5.0wt% BMF/PVA/GC (~221.8 kPa) is 12.7 times that of 0wt% BMF/PVA/GC water-based hydrogel (~17.5 kPa) and 7.4 times that of 0.5wt% BMF/PVA/GC water-based hydrogel (~30.0 kPa). This indicates that with the increase of BMF, the water-based hydrogel can withstand higher stress and have a larger elastic modulus, suggesting that BMF plays a crucial role in improving the mechanical properties of PVA/GC water-based hydrogel. These results indicate that BMF plays a critical role in enhancing the mechanical properties of the PVA/GC hydrogel, allowing it to withstand higher stress and exhibit larger elastic modulus. Furthermore, the results suggest that the BMF/PVA/GC hydrogel has excellent cyclic utilization and reusability properties.

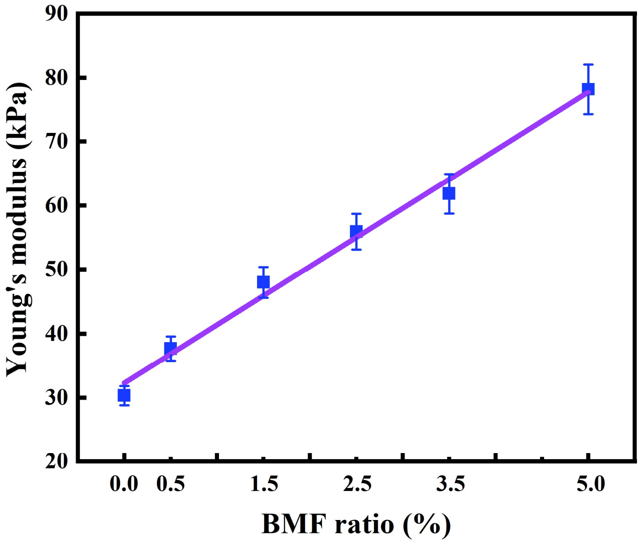

Figure 8. The variation of Young's modulus and BMF mass fraction.

Moreover, based on the aforementioned analysis, we have observed a linear relationship between the mass fraction of BMF in the PVA/GC/BMF hydrogel and the corresponding Young's modulus. Specifically, as the mass fraction of BMF increases, the mechanical performance of the PVA/GC/BMF hydrogel becomes stronger, as indicated by a higher value of Young's modulus. Building upon these findings, we compared the mass fractions of BMF in different hydrogels with their respective Young's modulus values and performed a fitting analysis. The resulting linear curve equation is given as follows:

$$y = 9087.08411x + 32281.31776$$

Here, y represents the magnitude of Young's modulus of the PVA/GC/BMF hydrogel in units of pascals (Pa), and x denotes the numerical value of the mass fraction of BMF in the hydrogel, measured in weight percentage (wt%). The fitting results were calculated with precision up to five decimal places.

3. Conclusions

In summary, we have developed a novel PVA/GC/BMF hydrogel with excellent mechanical properties and fatigue resistance through hydrogen-bonded crosslinking. Infrared spectroscopy and SEM analysis confirmed the hydrogen bonding interactions between PVA, GC, and BMF, where PVA and GC formed the first layer of flexible network through physical crosslinking, while PVA and BMF formed the second layer of rigid network through physical crosslinking. Low-cycle fatigue experiments demonstrated that the mechanical properties of the hydrogel can be quantitatively controlled by adjusting the mass fraction of BMF. Furthermore, the internally damaged PVA/GC/BMF hydrogel after 2000 cycles of compression could be reshaped and reused. Repeating the compression for an additional 2000 cycles on the reshaped PVA/GC/BMF hydrogel revealed that it retained certain mechanical properties and fatigue resistance, highlighting the value of such physically crosslinked DN hydrogels for cyclic applications.

Additionally, the mass fraction of BMF in the PVA/GC/BMF hydrogel exhibited a linear relationship with its mechanical properties, providing a controllable means to tailor the hydrogel's mechanical performance and achieve desired effects. The hydrogel demonstrated fatigue resistance and, notably, it not only retained its shape after repeated utilization but also could be recycled by melting and recasting under pressure, presenting a novel approach for secondary utilization of hydrogels.

Author Contributions: Conceptualization, Z.X.; methodology, D.L.; software, G.L. and W.H.; validation, Z.X. and J.D.; formal analysis, Y.Y.; investigation, Z.X and T.M.; resources, D.L; data curation,W.H. and W.X.; writing—original draft preparation, Y.Z. writing—review and editing, Y.Y. , Z.X.and W.X; All authors have read and agreed to the published version of the manuscript.

Funding: This research was funded by the Research Project of Research Center for Analysis and Measurement Kunming University of Science and Technology ,grant number 2021P20193103002.

Institutional Review Board Statement: Not applicable.

Informed Consent Statement: Not applicable.

Data Availability Statement: Details on all data supporting the reported results can be obtained in Tables 1–3 and Figures 1–9 of this original manuscript.

Conflicts of Interest: No potential conflict of interest was reported by the authors.

References

1. Lu, Y.; Yue, Y.; Ding,Q.; Mei,C.; Xu, X.; Wu, Q.; Xiao, H.; Han, J. Self-Recovery, Fatigue-Resistant, and Multifunctional Sensor Assembled by a Nanocellulose/Carbon Nanotube Nanocomplex-Mediated Hydrogel. *ACS. Appl Mater Inter*. **2021**, 42, 13.
2. Yang, F.; Zhao, J.; Koshut, W.J.; Watt, J.; Wiley, B.J. A Synthetic Hydrogel Composite with the Mechanical Behavior and Durability of Cartilage. *Adv. Funct Mater*. **2020**, 2003451.
3. Liu, T.; Peng, X.; Chen, Y.N.; Bai, Q.W.; Shang, C.; Zhang, L.; Wang, H. Hydrogen-Bonded Polymer–Small Molecule Complex es with Tunable Mechanical Properties. *Macromol. Rapid. Comm*. **2018**, 180, 0050.
4. Wen, N.; Jiang, B.; Wang, X.; Wang,X.J.; Shang, ZF ; Jiang, DW; Zhang, L ; Sun, CY ; Wu, ZJ ; Yan, H ; Liu, CT ; Guo, ZH . Overview of Polyvinyl Alcohol Nanocomposite Hydrogels for Electro-Skin, Actuator, Supercapacitor and Fuel Cell. *Chem. Rec*. **2020** ,8, 20.
5. Kerativitayanan, P.; Carrow, J. K.; Gaharwar, A. K. Nanomaterials for Engineering Stem Cell Responses. *Adv. Healthc, Mater*. **2015**, 4, 1600−1627.
6. Shi, S.J.; Peng, X.; Liu, T.Q.; Chen, Y.N.; He, C.C.; Wang, H.L. Facile preparation of hydrogen-bonded supramolecular polyvinyl alcohol-glycerol gels with excellent thermoplasticity and mechanical properties. *Polym. Int*. **2017**.
7. Yingkun, S.; Baohu, W.; Shengtong, S.; Peiyi, W. Aqueous spinning of robust, self-healable, and crack-resistant hydrogel microfibers enabled by hydrogen bond nanoconfinement. *Nat. Commun*. **2023**, 14, 1370.
8. Meng, X.H.; Qiao, Y.; Do, C.; Bras, W.; He, C.Y.; Ke, Y.B.; Russell, T.P.; Qiu, D. Hysteresis-Free Nanoparticle-Reinforced Hydrogels. Adv. Mater. **2021**, e2108243.
9. Xu, P.P.; Xu, H.X.; Yang, Y; Wang, X.L.; An, W.L.; Hu, Y.; Xu, SMA. nonswellable gradient hydrogel with tunable mechanical properties. *J Mater Chem. B*, **2020**, 8,13.
10. Dutta, A.; Das, R.K. Dual Cross-Linked Hydrogels with High Strength, Toughness, and Rapid Self-Recovery Using Dynamic Metal–Ligand Interactions. *Macromol Mater Eng*, **2019**, 8, 304.
11. Mu, Q.F.; Cui, K.P.; Wang, Z.J.; Matsuda, T.; Cui, W.; Kato, H.; Namiki, S.; Yamazaki, T.; Frauenlob, M.; Nonoyama, T.; Tsuda, M.; Tanaka, S.; Nakajima, T.; Gong, J.P. Force-triggered rapid microstructure growth on hydrogel surface for on-demand functions. *Nat. Commun.* **2022**, 13, 6213.
12. Xia, S.; Song, S.X.; Gao, G.H.Robust and flexible strain sensors based on dual physically cross-linked double network hydrogels for monitoring human-motion. *Chem Eng J* , **2018**, 354.
13. Wang, X.Q.; Chan, K.H.; Lu, W.H.; Ding, T.P.; Ng, S.W.L.; Cheng, Y.; Li, T.T.; Hong, M.H.; Tee, B.C.K.; Ho, G.W. Macromolecule conformational shaping for extreme mechanical programming of polymorphic hydrogel fibers. *Nat. Commun.* **2022**, 13, 3369.
14. Wang, T.T.; Wang, J.Q.; Li, Z.P.; Yue, M.Q.; Qing, X.L.; Zhang, P.X.; Liao, X.Z.; Fan, Z.J.; Yang, S.R.PVA/SA/MXene dual-network conductive hydrogel for wearable sensor to monitor human motions. *J Appl Polym Sci*, **2021**.
15. Xiao, G.; XinYu, D.; GuiJin, Z.; Huajian, G. Strong and tough fibrous hydrogels reinforc ed by multiscale hierarchical structures with multimechanisms. *Sci.Adv*. **2023**, 19, 2, 11.

16. Hua, M.; Wu, S. ;Ma, Y.; Zhao, Y.; Chen, Z.; Frenkel, I.; Strzalka, J.;Zhou, H.;Zhu, X.; He, X. Strong tough hydrogels via the synergy of freeze-casting and salting out. *Nature* **2021**, 590, 594–599.
17. Liang, X.; Chen, G.; Lin, S.;Zhang, J.; Wang, L.; Zhang, P.; Wang, Z.;Wang, Z.; Lan, Y.; Ge,Q.; Liu, J. Anisotropically fatigue-resistant hydrogels. *Adv. Mater.* **2021**, 33, 210.
18. Conley, G.M.; Zhang, C.; Aebischer, P.; Harden, J.L.; Scheffold, F. Relationship between rheology and structure of interpenetrating, deforming and compressing microgels. Nat. Commun. 2019, 10, 2436.
19. Wang, X.; Qiu, Y.; Chen, G.; Chu, Z. , Zhu, Z. Self-healable poly(vinyl alcohol) photonic crystal hydrogel. ACS Applied Polymer Materials, 2020, 2, 5, 2086-2092.
20. Truong,N. F.; Kurt,E.; Tahmizyan,N.; Lesher-Pérez, S.C.; Chen,M.; Darling, N. J.; Xi,W.; Segura,T. Microporous annealed particle hydrogel stiffness, void space size, and adhesion properties impact cell proliferation, cell spreading, and gene transfer. Acta Biomater. 2019, 94, 160–172.
21. Morikawa, Y.; Yamagiwa, S.; Sawahata, H.; Numano, R.; Koida, K.; Ishida, M.; Kawano, T. Ultrastretchable kirigami bioprobes. Adv. Healthc. Mater. 2018, 7, 1701100.
22. Gong, J.P. Why are double network hydrogels so tough? Soft Matter **2010**, 6, 2583–2590.
23. Haraguchi, K.; Takehisa, T.; Fan, S. Effects of clay content on the properties of nanocomposite hydrogels composed of poly (N-isopropylacrylamide) and clay. Macromolecules **2002**, 35, 10162–10171.
24. Liang, S.; Wu, Z.L.; Hu, J.; Kurokawa, T.; Yu, Q.M.; Gong, J.P. Direct observation on the surface fracture of ultrathin film double-network hydrogels. Macromolecules **2011**, 44, 3016–3020.
25. Kim, Y.S.; Liu, M.; Ishida, Y.; Ebina, Y.; Osada, M.; Sasaki, T.; Hikima, T.; Takata, M.; Aida, T. Thermoresponsive actuation enabled by permittivity switching in an electrostatically anisotropic hydrogel. Nat. Mater. **2015**, 14, 1002–1007.
26. Huang, X.; Ge, G.; She, M.; Ma, Q.; Lu, Y.; Zhao, W.; Shen, Q.; Wang, Q.; Shao, J. Self-healing hydrogel with multiple dynamic interactions for multifunctional epidermal sensor. Appl. Surf. Sci. **2022**, 598, 153803.
27. Xin, H. Double-Network Tough Hydrogels: A Brief Review on Achievements and Challenges. Gels 2022, 8, 247.
28. Nonoyama, T.; Wada, S.; Kiyama, R.; Kitamura, N.; Mredha, M.T.I.; Zhang, X.; Kurokawa, T.; Nakajima, T.; Takagi, Y.; Yasuda, K. Double-network hydrogels strongly bondable to bones by spontaneous osteogenesis penetration. Adv. Mater. **2016**, 28, 6740–6745.
29. Arakaki, K.; Kitamura, N.; Fujiki, H.; Kurokawa, T.; Iwamoto, M.; Ueno, M.; Kanaya, F.; Osada, Y.; Gong, J.P.; Yasuda, K. Artificial cartilage made from a novel double-network hydrogel: In vivo effects on the normal cartilage and ex vivo evaluation of the friction property. J. Biomed. Mater. Res. Part A Off. J. Soc. Biomater. Jpn. Soc. Biomater. Aust. Soc. Biomater. Korean Soc. Biomater. **2010**, 93, 1160–1168.
30. Sun, J.-Y.; Zhao, X.; Illeperuma, W.R.; Chaudhuri, O.; Oh, K.H.; Mooney, D.J.; Vlassak, J.J.; Suo, Z. Highly stretchable and tough hydrogels. Nature **2012**, 489, 133–136.
31. Sun, Y.N.; Gao, G.R.; Du, G.L.; Cheng, Y.J.; Fu, J. Super Tough, Ultrastretchable, and Thermoresponsive Hydrogels with Functionalized Triblock Copolymer Micelles as Macro-Cross-Linkers. ACS Macro. Lett. **2014**, 3, 496–500.
32. Chaudhuri, O.; Gu, L.; Darnell, M.; Klumpers, D.; Bencherif, S.A.; Weaver, J.C.; Huebsch, N.; Mooney, D.J. Substrate stress relaxation regulates cell spreading. Nat. Commun. **2015**, 6, 6365.
33. Cacopardo, L.; Guazzelli, N.; Nossa, R.; Mattei, G.; Ahluwalia, A. Engineering hydrogel viscoelasticity. J. Mech. Behav. Biomed. Mater. **2019**, 89, 162–167.
34. Zhao, X.; Chen, X.; Yuk, H.; Lin, S.; Liu, X.; Parada, G. Soft Materials by Design: Unconventional Polymer Networks Give Extreme Properties. Chem. Rev. **2021**, 121, 4309–4372.
35. Wang, Z.J.; Jiang, J.; Mu, Q.; Maeda, S.; Nakajima, T.; Gong, J.P. Azo-Crosslinked Double-Network Hydrogels Enabling Highly Efficient Mechanoradical Generation. J. Am. Chem. Soc. **2022**, 144, 3154–3161.
36. Millereau, P.; Ducrot, E.; Clough, J.M.; Wiseman, M.E.; Brown, H.R.; Sijbesma, R.P.; Creton, C. Mechanics of elastomeric molecular composites. Proc. Natl. Acad. Sci. USA **2018**, 115, 9110–9115.
37. Gong, J.P. Materials both tough and soft. Science **2014**, 344, 161–162.
38. Bin Imran, A.; Esaki, K.; Gotoh, H.; Seki, T.; Ito, K.; Sakai, Y.; Takeoka, Y. Extremely stretchable thermosensitive hydrogels by introducing slide-ring polyrotaxane cross-linkers and ionic groups into the polymer network. Nat. Commun. **2014**, 5, 5124.
39. Gong, J.P.; Katsuyama, Y.; Kurokawa, T.; Osada, Y. Double-network hydrogels with extremely high mechanical strength. Adv. Mater. **2003**, 15, 1155–1158.
40. Choi, S.; Choi, Y.; Kim, J. Anisotropic hybrid hydrogels with superior mechanical properties reminiscent of tendons or ligaments. Adv. Funct. Mater. **2019**, 29, 1904342.
41. Yang, Y.; Wang, X.; Yang, F.; Shen, H.; Wu, D. A Universal Soaking Strategy to Convert Composite Hydrogels into Extremely Tough and Rapidly Recoverable Double-Network Hydrogels. Adv. Mater. **2016**, 28, 7178–7184.
42. Yu, J.; Xu, K.; Chen, X.; Zhao, X.; Yang, Y.; Chu, D.; Xu, Y.; Zhang, Q.; Zhang, Y.; Cheng, Y. Highly Stretchable, Tough, Resilient, and Antifatigue Hydrogels Based on Multiple Hydrogen Bonding Interactions Formed by Phenylalanine Derivatives. Biomacromolecules **2021**, 22, 1297–1304.

43. Ahmed, S.; Nakajima, T.; Kurokawa, T.; Haque, M.A.; Gong, J.P. Brittle–ductile transition of double network hydrogels: Mechanical balance of two networks as the key factor. Polymer **2014**, 55, 914–923.
44. Chen, G.; Tang, W.W.; Wang, X.H.; Zhao, X.L.; Chen, C.; Zhu, Z.G. Applications of Hydrogels with Special Physical Properties in Biomedicine. Polymers **2019**, 11, 1420.
45. Darabi, M.A.; Khosrozadeh, A.; Mbeleck, R.; Liu, Y.; Chang, Q.; Jiang, J.; Cai, J.; Wang, Q.; Luo, G.; Xing, M. Skin-Inspired Multifunctional Autonomic-Intrinsic Conductive Self-Healing Hydrogels with Pressure Sensitivity, Stretchability, and 3D Printability. Adv. Mater. **2017**, 29, 1700533.
46. Cui, K.; Sun, T.L.; Liang, X.; Nakajima, K.; Ye, Y.N.; Chen, L.; Kurokawa, T.; Gong, J.P. Multiscale energy dissipation mechanism in tough and self-healing hydrogels. Phys. Rev. Lett. **2018**, 121, 185501.
47. Cao, J.; Li, J.; Chen, Y.; Zhang, L.; Zhou, J. Dual Physical Crosslinking Strategy to Construct Moldable Hydrogels with Ultrahigh Strength and Toughness. Adv. Funct. Mater. **2018**, 28, 1800739.
48. Han, L.; Yan, L.; Wang, K.; Fang, L.; Zhang, H.; Tang, Y.; Ding, Y.; Weng, L.-T.; Xu, J.; Weng, J. Tough, self-healable and tissue-adhesive hydrogel with tunable multifunctionality. NPG Asia Mater. **2017**, 9, e372.
49. Samp, M.A.; Iovanac, N.C.; Nolte, A.J. Sodium Alginate Toughening of Gelatin Hydrogels. ACS Biomater. Sci. Eng. **2017**, 3, 3176–3182.
50. Fan, H.; Wang, J.; Jin, Z. Tough, Swelling-Resistant, Self-Healing, and Adhesive Dual-Cross-Linked Hydrogels Based on Polymer–Tannic Acid Multiple Hydrogen Bonds. Macromol. **2018**, 51, 1696–1705.
51. El Salmawi, K.M. Gamma radiation-induced cross-linked PVA/chitosan blends for wound dressing. J. Macromol. Sci. Part A-Pure Appl. Chem. **2007**, 44, 541–545.
52. Wang, Z.; Zheng, X.; Ouchi, T.; Kouznetsova, T.B.; Beech, H.K.; Av-Ron, S.; Matsuda, T.; Bowser, B.H.; Wang, S.; Johnson, J.A.; et al. Toughening hydrogels through force-triggered chemical reactions that lengthen polymer strands. Science **2021**, 374, 193–196.
53. Fei, C.; Huang, D.; Feng, S. Adsorption behavior of amphoteric double-network hydrogel based on poly(acrylic acid) and silica gel. J. Polym. Res. **2012**, 19, 1–7.
54. Mansur, H.S.; Sadahira, C.M.; Souza, A.N.; Mansur, A.A. FTIR spectroscopy characterization of poly (vinyl alcohol) hydrogel with different hydrolysis degree and chemically cross-linked with glutaraldehyde. Mater. Sci. Eng. C-Biomim. Supramol. Syst. **2008**, 28, 539–548.
55. Lin, S.; Liu, J.; Liu, X.; Zhao, X. Muscle-like fatigue-resistant hydrogels by mechanical training. Proc. Natl. Acad. Sci. USA **2019**, 116, 10244–10249.
56. Wang, P.; Wu, M.; Li, R.; Cai, Z.; Zhang, H. Fabrication of a Double-Network Hydrogel Based on Carboxymethylated Curdlan/Polyacrylamide with Highly Mechanical Performance for Cartilage Repair. ACS Appl. Polym. Mater. **2021**, 3, 5857–5869.
57. Ma, M.Y.; Liu, S.H.; Chen, S.F. Strong double network hydrogels reinforced by silk fibroin microfibers. J. Chem. Eng. Chin. Univ. **2021**, 35, 148–154.
58. Li, S.; Wang, X.; Zhu, J.; Wang, Z.; Wang, L. Preparation and characterization of double network hydrogel with high-strength and self-healing. Mater. Today Commun. **2021**, 27, 102450.
59. Kimura, T.; Urayama, K. Multiaxial stress relaxation of dual-cross-link Poly(vinyl alcohol) hydrogels. ACS Macro Lett. **2019**, 9, 1–6.
60. Majmudar, T.S.; Behringer,R. P. Contact force measurements and stress-induced anisotropy in granular materials. Nat. **2005**, 435, 1079–1082.
61. Seiffert,S.; Weitz,D.A. Microfluidic fabrication of smart microgels from macromolecular p re cursors. Polym. **2010**, 51, 5883–5889.
62. Nasrollahzadeh, N.; Karami, P.; Pioletti, D.P. Control of Dissipation Sources: A Central Aspect for Enhancing the Mechanical and Mechanobiological Performances of Hydrogels. *ACS App Mater & Inter*, **2019**.
63. Lu, Y.; Yue, Y.Y.; Ding, Q.Q.; Mei, C.T.; Xu, X.W.; Wu, Q.L.; Xiao, H.N.; Han, J.Q. Self-Recovery, Fatigue-Resistant, and Multifunctional Sensor Assembled by a Nanocellulose/Carbon Nanotube Nanocomplex-Mediated Hydrogel. *ACS App Mater & Inter*, **2021**, 42, 13.
64. Zhang, F.; Xiong, L.G.; Ai, Y.J.; Liang, Z.; Liang, Q.L. Stretchable Multiresponsive Hydrogel with Actuatable, Shape Memory, and Self-Healing Properties. *Adv. Sci*, **2018**, 5, 8.
65. Young,D. A.; Ibrahim,D. O.; Hu,D.; Christman, K.L. Injectable hydrogel scaffold from decellularized human lipoaspirate. *Acta Biomater*. **2011**, 7, 1040–1049.
66. Nurazzi, N.M.; Harussani, M.M.; Aisyah, H.A.; Ilyas, R.A.; Norrrahim, M.N.F.; Khalina, A.; Abdullah, N. Treatments of natural fiber as reinforcement in polymer composites—A short review. *Funct. Compos. Struct.* **2021**, 3, 024002.
67. Guo, X.W; Li, J.; Wang, J.X.; Huang, L.Q.; Cheng, G.J.; Zhang, Q.; Zhu, H.; Zhang, M.Y.; Zhu, S.P. Stretchable Hydrogels with Low Hysteresis and High Fracture Toughness for Flexible Electronics. *Macromol Rapid Comm*, **2022**, 43, 4, e21007,16.
68. Hossain, S.I.; Hasan, M.; Hasan, M.N.; Hassan, A. Effect of chemical treatment on physical, mechanical and thermal properties of ladies finger natural fiber. *Adv. Mater. Sci. Eng*. **2013**, 2013, 824274.

69. Wang, Y.; Yu, X.; Li, Y.; Zhang, Y.; Geng, L.; Shen, F.; Ren, J. Hydrogelation Landscape Engineering and a Novel Strategy to Design Radically Induced Healable and Stimuli-Responsive Hydrogels. ACS Appl. Mater. Interfaces **2019**, 11, 19605–19612.
70. Chen, L.; Tian, Y.; Tong, Q.; Zhang, Z.; Jin, Z. Effect of Pullulan on the Water Distribution, Microstructure and Textural Properties of Rice Starch Gels during Cold Storage. *Food Chem*. **2017**, 214, 702–709.
71. Gong, J. P. Why are Double Network Hydrogels so Tough. *Soft Matter.* **2010**, 6, 2583–2590.
72. Yang, Y.; Wang, X.; Yang, F.; Shen, H.; Wu, D. A Universal Soaking Strategy to Convert Composite Hydrogels into Extremely Tough and Rapidly Recoverable Double-Network Hydrogels. *Adv. Mater*. **2016**, 28, 7178–7184.
73. Figueiredo, P.; Lintinen, K.; Hirvonen, J. T.; Kostiainen, M. A.; Santos, H. A. Properties and Chemical Modifications of Lignin: towards Lignin-based Nanomaterials for Biomedical Applications. Prog. *Mater. Sci.* **2018**, 93, 233–269.
74. Salvati, E; Brandt, LR; Uzun, F ; Zhang, H ; Papadaki, C ; Korsunsky, AM. Multiscale analysis of bamboo deformation mechanisms following NaOH treatment using X-ray and correlative microscopy. *Acta Biomater,* **2018**.
75. Xie, J.L.; Hse, C.Y; De Hoop, C.F.; Hu, T.X.; Qi, J.Q.; Shupe, T.F. Isolation and characterization of cellulose nanofibers from bamboo using microwave liquefaction combined with chemical treatment and ultrasonication. *Carbohydr. Polym*. **2016**, 151, 725-734.
76. Yuan, Z.; Wei, W.; Wen, Y.; Improving the production of nanofibrillated cellulose from bamboo pulp by the combined cellulase and refining treatment. *J Chemical Tech & Biotech*. **2019**.
77. Wu, Y.; Wu, X.Y.; Shi, T.L.; Chen, H.; Wang, H.K.; Sun, M.; Zhang, J.L. The Microstructure and Mechanical Properties of Poplar Catkin Fibers Evaluated by Atomic Force Microscope (AFM) and Nanoindentation. *Forests*, **2019**, 10, 11, 938.
78. Khalil, H.; Bhat, I.; Jawaid, M.; Zaidon, A.; Hermawan, D.; Hadi, Y.S. Bamboo fibre reinforced bio composites: a review. *Materi & Des.* **2012**, , 42, 353-368.
79. Rosa, M.F.; Chiou, B.S.; Medeiros, E.S.; Wood, D.F.; Williams, T.G.; Mattoso, L.H.C.; Orts, W.J.; Imam, S.H. Effect of fiber treatments on tensile and thermal properties of starch/ethylene vinyl alcohol copolymers/coir biocomposites. *Bioresour. Technol.* **2009**, 100, 5196–5202.
80. Faruk, O.; Bledzki, A.K.; Fink, H.P.; Sain, M. Biocomposites reinforced with natural fibers: 2000–2010. *Prog. Polym. Sci.* **2012**, 11, 37.
81. Gratani, L.; Crescente, M.F.; Varone, L.; Fabrini, G.; Digiulio, E. Growth pattern and photosynthetic activity of different bamboo species growing in the Botanical Garden of Rome Flora - Morphology, Distribution, *Funct. Ecolo. Plan.* **2008**, 1, 203, 77-84.
82. Sanjay, M.R.; Arpitha, G.R.; Yogesha, B. Study on Mechanical Properties of Natural - Glass Fibre Reinforced Polymer Hybrid Composites: A Review. Materi. Tod. Procee. **2015**, 2, 2959-2967.
83. Krishnaiah, P.; Manickam, S.; Ratnam, C.T.; Raghu, M.S.; Parashuram, L.; Prashantha, K.; Jeon, B.H. Surface-treated short sisal fibers and halloysite nanotubes for synergistically enhanced performance of polypropylene hybrid composites. J. Thermoplast. Compos. Mater. **2020**, 0892705720946063.
84. Yusoff, R.B.; Takagi, H.; Nakagaito, A.N. "Tensile and flexural properties of polylactic acid-based hybrid green composites reinforced by kenaf, bamboo and coir fibers." *Industl Crop & Pro.* **2016**, 94, 562-573.
85. Soutis, C. Carbon fiber reinforced plastics in aircraft construction. *Mater. Sci. Eng. A*. **2005**, 412, 171-176.
86. Mousavi, S.R.; Zamani, M.H.; Estaji, S.;Tayouri, M.I.; Arjmand, M.; Jafari, S.H.; Nouranian, S.; Khonakdar, H.A. Mechanical properties of bamboo fiber-reinforced polymer composites: a review of recent case studies. *J Mater Sci.* **2022**, 57, 3143–3167.
87. Ismail, H.; Edyham, M.R.; Wirjosentono, B. Bamboo fibre filled natural rubber composites: The effects of filler loading and bonding agent. *Polym Test*, **2002**, 21, 2, 139-144.
88. Nurazzi, N.M.; Asyraf, M.R.M.; Rayung, M.; Norrrahim, M.N.F.; Shazleen, S.S.; Rani, M.S.A.; Shafi, A.R.; Aisyah, H.A.; Radzi, M.H.M.; Sabaruddin, F.A.; Ilyas, R.A.; Zainudin, E.S.; Abdan, K. Thermogravimetric Analysis Properties of Cellulosic Natural Fiber Polymer Composites: A Review on Influence of Chemical Treatments. *Polym*. **2021**, 13, 2710.
89. Okubo, K.; Fujii, T.; Yamamoto, Y. Development of bamboo-based polymer composites and their mechanical properties. *Compos Part A-Appl S*. **2004**, 35, 3, 377-383.
90. Thwe, M.M.; Liao, K. Effects of environmental aging on the mechanical properties of bamb oo-glass fiber reinforced polymer matrix hybrid composites. *Compos Part A-Appl S.* **2002**, 33, 43–52.
91. Shih, Y.F. Mechanical and thermal properties of waste water bamboo husk fiber reinforced epoxy composites. *Mater Sci & Eng A*, **2007**, 445 , 289-295.
92. Guimaraes, M.; Botaro, V.R.; Novack, K.M.; Teixeira, F.G.; Tonoli, G.H.D.Starch/PVA-based nanocomposites reinforced with bamboo nanofibrils ,*Ind Crop Prod*, **2015**, 70, 72-83.
93. Asyraf, M.R.M.; Ishak, M.R.; Sapuan, S.M.; Yidris, N. Influence of Additional Bracing Arms as Reinforcement Members in Wooden Timber Cross-Arms on Their Long-Term Creep Responses and Properties. *Appl. Sci*. **2021**, 11, 2061.

94. Zhang, X., Yu, Y., Jiang, Z.; Wang, H. The effect of freezing speed and hydrogel concentration on the microstructure and compressive performance of bamboo-based cellulose aerogel, Journal of Wood Science, **2015**, 61, 6, (595-601).
95. Xu, K.; Narayanan, K.; Lee, F.; Bae, K.H.; Gao, S.; Kurisawa, M. Enzyme-mediated hyaluronic acid–tyramine hydrogels for the propagation of human embryonic stem cells in 3D. *Acta Biomater*. **2015**, 24, 159–171.
96. Nguyen, D.D.; Vu, C.M.; Vu, H.T.; Choi, H.J. Micron-size white bamboo fibril-based silane cellulose aerogel: Fabrication and oil absorbent characteristics , *Mater*, 12, 9, **2019**.
97. Norul Izani, M.A.; Paridah, M.T.; Anwar, U.M.K.; Mohd Nor, M.Y.; H'Ng, P.S. Effects of fiber treatment on morphology, tensile and thermogravimetric analysis of oil palm empty fruit bunches fibers. Compos. Part B Eng. **2013**, 45, 1251–1257.
98. Jiang, S.; Liu, S.; Feng, W. PVA Hydrogel Properties for Biomedical Application. *J. Mech. Behav. Biomed. Mater*. **2011**, 4, 1228–1233.
99. Hassan, C. M.; Peppas, N. A. Structure and Morphology of Freeze/Thawed PVA Hydrogels. *Macromolecules*. **2000**, 33, 2472– 2479.